Microelectronic Engineering 170 (2017) 44–48

Contents lists available at ScienceDirect

Microelectronic Engineering

journal homepage: www.elsevier.com/locate/mee

Research paper

Synthesis and field emission characteristics of W_5O_{14} nanowires film

G. Ulisse [a,*], C. Ciceroni [a], A.D. Carlo [a], F. Brunetti [a], J. Jelenc [b], M. Saqib [b], A. Varlec [b], M. Remskar [b]

[a] Department of Electronic Engineering, University of Rome Tor Vergata, Rome, 00133, Italy
[b] Solid State Physics Department, Jozef Stefan Institute, Ljubljana, 1000, Slovenia

ARTICLE INFO

Article history:
Received 6 October 2016
Received in revised form 25 November 2016
Accepted 24 December 2016
Available online 29 December 2016

Keywords:
Field emission
Nanowire
Nanoelectronics

ABSTRACT

The W_5O_{14} nanowires are metallic oxides with specific resistivity of 27 μΩcm and diameters bellow 100 nm. The field emission characteristics of the films composed of these nanowires have been investigated. The emitting current densities up to 6.4 mA/cm^2 have been obtained at very low electric field of about 3 V/μm. The samples were allowed to emit for more than 100 h without showing significant decays of the emitting current and without substantial current oscillations. These characteristics make these nanowires very promising for the realization of large area field emitting cathodes.

1. Introduction: the manuscript

Field emission cathodes can be used in different applications such as field emission display, portable x-ray generators, microwave sources and amplifiers [1–4]. Many field emission studies have been performed on nanostructures, such as carbon nanotubes, metallic or semiconductive nanowires [5–7]. In particular carbon nanotubes (CNTs), have been extensively studied in the last twenty years for their excellent field emission properties due to their very high aspect ratio, the low-voltage emission, the robustness [8–9]. In the last decade some investigations have been performed on tungsten oxide nanowires including WO_2, WO_3, $W_{18}O_{49}$ as a possible alternative to CNTs field emitters [10–12]. In particular $W_{18}O_{49}$ exhibits good field-emission characteristics. Field emission measurements on a single W_5O_{14} nanowire have been performed demonstrating that these nanowires have all the properties required from a good field emitter [13]. In this work we performed a complete study about the field emission characteristics of W_5O_{14} nanowires film in order to verify the possibility of use them in a real device with large emitting area. The main parameter to define the quality of field emitters is the field enhancement factor. In order to extrapolate this value from the I—V characteristics it is necessary to know the work function of the emitters [14]. The work function of the W_5O_{14} nanowires has been then measured by Kelvin microscopy in non contact atomic force microscopy (UHV-AFM Omicron). Long stability measurements of over 100 h have been done to demonstrate the robustness of such nanoemitters that is completely comparable with carbon nanotubes.

W_5O_{14} nanowires have been synthesized by iodine transport method [15] using nickel as a growth promoter and WO_3 as source of tungsten and oxygen. The starting material consisted of: 352.7 mg WO_3 powder (Sigma Aldrich, 99.99%), 37.5 mg nickel (mechanically cut metal foil) and 567 mg iodine (1–3 mm beads, Sigma Aldrich, 99.7%) was evacuated in quartz ampoule, sealed and put into two zone furnace. The temperature was increased for 24 h from room temperature to the working conditions. Material was transported from the hot zone (860 °C) to the cold zone at (736 °C) of the furnace under 6.2 °C/cm temperature gradient. Transport reaction run for 500 h and then cooled down under 35°/h cooling rate. Transported material of deep blue color consisted of long, rigid nanowires that tend to clump into bundles. X-ray diffraction spectrum (Fig. 1) reveals a pure W5O14 crystal phase according to the tetragonal W_5O_{14} crystals with lattice constants: a = 2.333 nm and c = 0.3797 nm (JCPDS No. 41-0745). A relatively low (001) peak in the spectrum, which is in bulk W4O14 the most intensive, is explained by the geometry where majority of the nanowires, which are grown along [001] direction, lay flat on the plastelin used for the sample fixing onto the XRD holder. A peak at 29.2° belongs to the plastelin (labeled with *).

The SEM image of the W_5O_{14} pressed film (Fig. 2a) shows that majority of the nanowires are randomly oriented along the film surface. Their density is relatively uniform at a large area. Length of the nanowires exceeds several tens of μm while their diameter is around 100 nm. The nanowires are very rigid and of homogeneous diameter along their length. They agglomerate into rare, weakly bonded bundles composing of a few nanowires. Scanning tunneling microscopy (Fig. 2b) reveals surface corrugation with a few nm deep channels along the nanowire. The work function (WF) of the nanowires has been determined by Kelvin microscopy in non contact atomic force microscopy operating in ultra high vacuum (UHV). This method is

* Corresponding author.

http://dx.doi.org/10.1016/j.mee.2016.12.026
0167-9317/

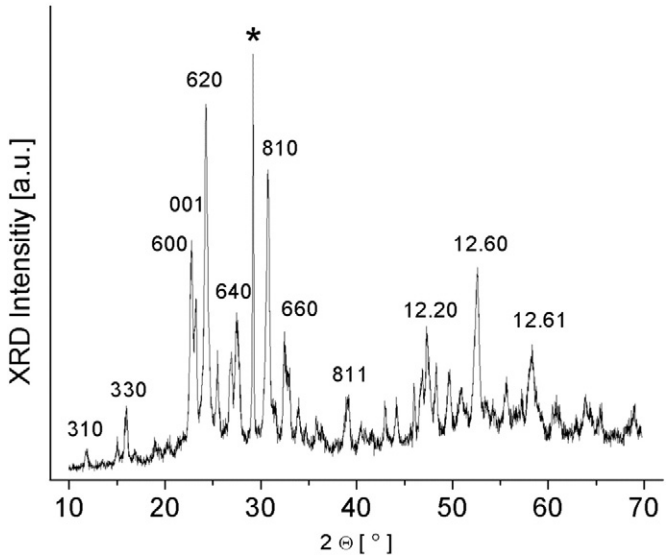

Fig. 1. X-ray diffraction pattern of the W5O14 nanowires indexed in accordance with JCPDS No. 41-0745.

based on a measurement of the electrostatic forces between the AFM tip and a nanowire under applied frequency modulation [16]. Due to electrostatic forces the first resonant frequency of the cantilever is lowered when tip approaches sample. This frequency shift is linearly dependent on tip-sample distance; therefore it can be used as its control. The experiments were performed at −40 Hz. At a certain frequency shift, an alternative (a.c.) voltage, Ua.c. = 0.7 V; ω = 2 kHz in our case, was applied to the AFM tip causing oscillation of the electrostatic forces. A lock-in amplifier was tuned to the frequency (ω). A superimposed d.c. voltage ($U_{d.c.}$) on the AFM tip was adjusted so that the response on the lock-in amplifier at the frequency ω became zero. Under this condition $U_{d.c.}$ is equal to the contact potential difference (CPD) between AFM tip and the sample. The CPD reveals difference in their work functions. Because unknown work function of AFM tip, the W5O14 nanowire were put on HOPG crystal and the contact potential difference was measured simultaneously on the W5O14 nanowires and on HOPG. Knowing work function of HOPG this method enables to calculate work function of measured W5O14 nanowires. Several measurements have been performed on different nanowires. The WF values of nanowires were different from a nanowire to nanowire, but always lower than the WF measured on graphite (4.6 eV). The values from 4.23 to 4.36 eV were obtained on single W_5O_{14} nanowires put on HOPG (Fig. 2c, d). These values are lower than work function of carbon nanotubes (4,95–5,05 eV) [17] or (4.7–4,9 eV) [18]. They are comparable to pure tungsten crystals, where work function strongly depends on a particular emission plane and ranges from 5.25 eV (110 plane) to 4,47 eV (111 plane) [19], but which increases by trace oxygen to 4,9 eV [20]. Work function of WO_3 is 4.8 eV [21]. Low work function

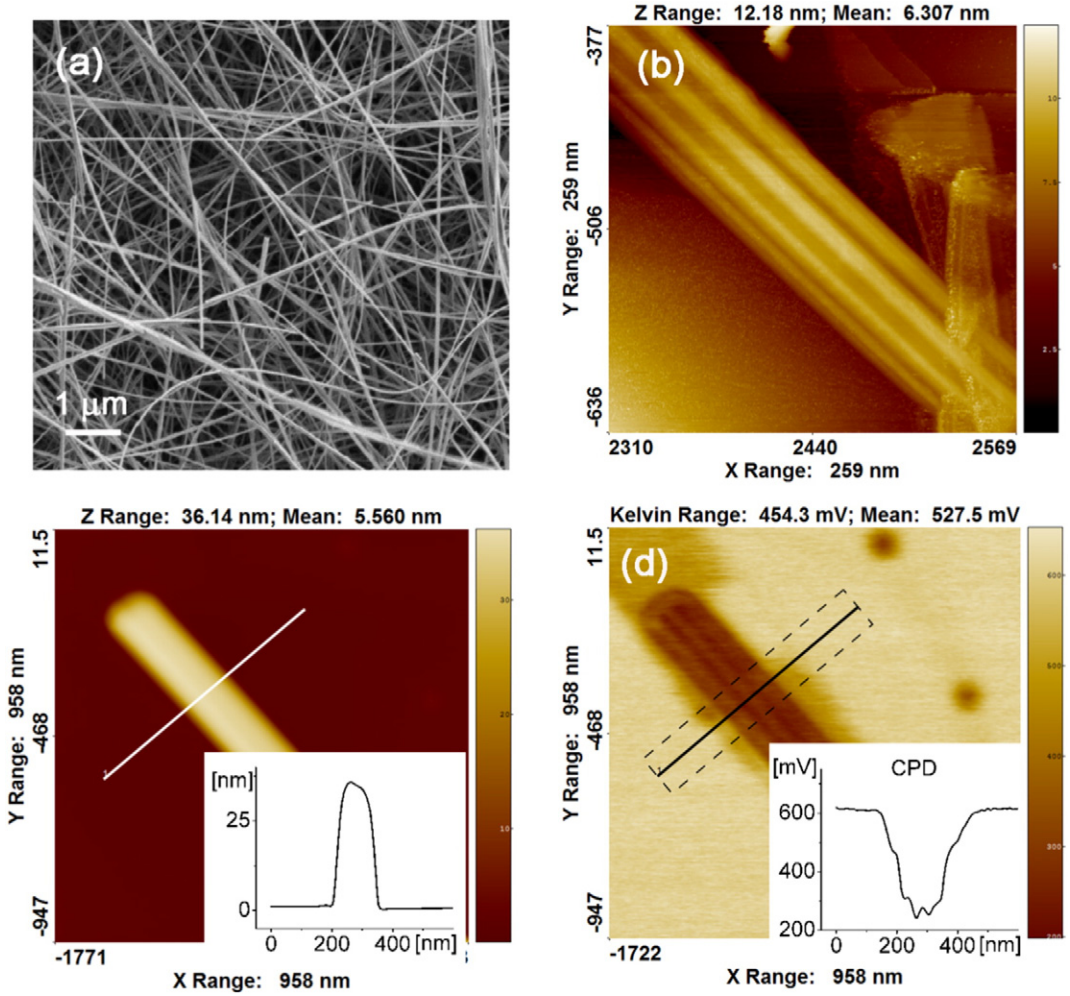

Fig. 2. The W_5O_{14} nanowires: a) SEM topography with in-plane random oriented nanowires; b) Scanning tunneling microscopy (STM) image revealing surface corrugation on a single nanowire; c) Non-contact AFM image of a single 35 nm thick W_5O_{14} nanowire with a line profile (inset); d) The corresponding Kelvin image ($U_{a.c.}$ = 0.7 V; ω = 2 kHz) with the contact potential difference profile (inset).

is advantage in the field emission phenomena since it helps in extraction of electrons from the emitters.

The field emission measurements were performed in a vacuum chamber at a vacuum level of 10^{-7} mbar. The W_5O_{14} nanowires were pressed together to form a stiff, self-standing film for the field emission testing. The W_5O_{14} films glued on metallic substrates with conductive silver paste, have represented cathodes in the diode configuration of the measurements. The W_5O_{14} cathodes were mounted on a sample holder that can be moved in the x-y plane trough two stepper motors. The anode was a metallic round tip that has a diameter of 1 mm; it can be moved with a stepper motor along the z axis with minimum steps of 50 nm. During measurements, the anode-cathode distance was maintained fixed at 500 μm. A programmable voltage source (Keithley 248) was used for applying voltage onto the anode in a range up to 5 kV. The emitted current was measured with a picoammeter (Keithley 6485) that has a range from 2 nA to 20 mA. A protection circuit was electrically connected between the cathode and the picoammeter to avoid electrical discharge that could damage the instrument. For the calculation of the current density, we considered the anode surface as an area of a circle with 1 mm diameter, i.e. $7.85 \cdot 10^{-3}$ cm^2, this value is not exactly the same of the emitting area but it can be used as first approximation to have the order of magnitude of the emitted current density.

Before the characterization, a conditioning process of the nanowires has been performed to remove adsorbates [22]. A possible procedure that can facilitate the desorption of impurities involves the application of appropriate voltages for specific time intervals. The sample was then measured continuously for 5 h at an anode voltage of 1600 V (Fig. 3a). At the beginning of the process, the emitting current has increased significantly up to a stable value of about 45 μA with low current oscillations after approximately 100 min of the emission. The average current was 44 μA with a standard deviation of just 2 μA. The current-voltage (I—V) measurements have been then performed with anode voltage sweep.

The emitted current showed very good stability and reproducibility. The two curves in Fig. 3b have been measured at different time and sweeping the anode voltage up (black line) and down (red line). The I—V measurements were performed for several hours and the maximum current varied no more than ± 2 μA around 48 μA.

Two different samples prepared in the same way as described above have been measured. A maximum current density of 6.4 mA/cm^2 at 3.2 V/μm electric field has been obtained for the first sample and 0.5 mA/cm^2 at 2 V/μm for the second one. In order to calculate the field enhancement factor the I—V curve can be described in the Fowler-Nordheim plot where $\ln(I/V^2)$ is plotted as function of 1/V (see Fig. 4). Analyzing this plot the field enhancement factor can be

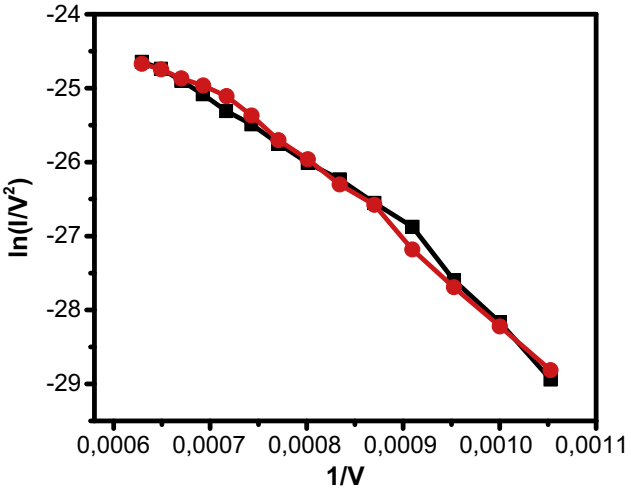

Fig. 4. Fowler Nordheim plot.

calculated with the following formula.

$$\beta = \frac{-B_f \cdot d \cdot \varphi^{1.5}}{m} \quad (1)$$

where 'd' the anode cathode distance, 'β' is the field enhancement factor and 'φ' is the emitters work function and 'm' is the slope of the Fowler-Nordheim plot.

Considering an average work function of 4.3 eV obtained from the Kelvin measurements, the field enhancement factor of about 3910 ± 65 and 4200 ± 176 were calculated, respectively. These values are much higher than the typical values obtained with carbon nanotubes (1000 − 2000) [23]. There could be several factors that can justify this high enhancement factor. The field enhancement factor can depend from several parameters such as shape, geometrical dimensions, distribution and cathode anode distance. Typically CNTs have a eight of 1–2 μm and radius than can be from 1 to 2 nm up to few tenths of nm. In our case the length of the nanowires is in the order of some tenths of μm and this could be a factor that cause the high enhancement factor. The field enhancement factor can also slightly increase with the increase of the anode-cathode distance [25,26]. In the measurements a quite big anode-cathode distance of 0.5 mm was used and this can produce a further increase, even if small, of the enhancement factor.

A long time stability measurement has been then performed to verify the durability of such cathode: the field emission was

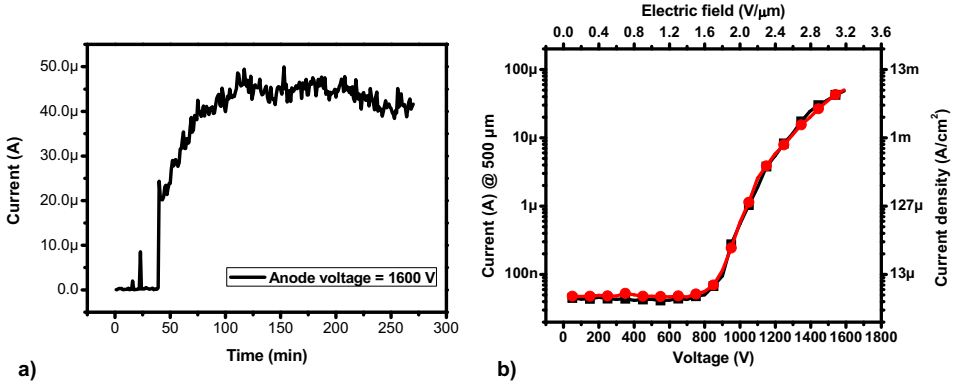

Fig. 3. a) Time evolution of the activation process of the emission performed at 1600 V; b) Current-voltage characteristics under voltage ramp up to 1600 V and the corresponding current density as a function of electric field.

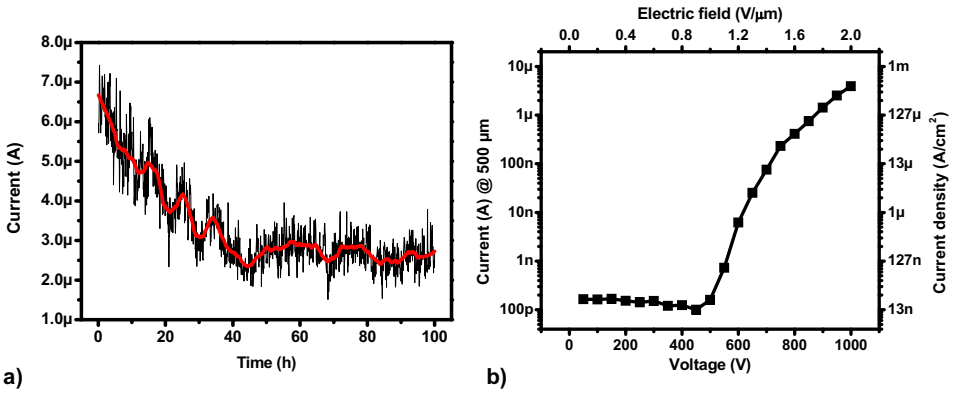

Fig. 5. a) Time evolution of the emitted current from W_5O_{14} nanowires during long time stability test, b) I—V characteristics after the long time stability test

measured for 100 h at the anode voltage of 850 V (Fig. 5a). The current was decreasing in the first 40 h, but then it became stable at an average value of 2.4 μA, with a standard deviation of 300 nA, for the remaining 60 h. A starting emitting current density of 1 mA/cm^2 was considered for the stability measurements since it is usually considered for some application like field emission display or X-ray generators. The current decreased up to about 0.3 mA/cm^2 and remained stable at that value that can be still very interesting for the application mentioned above. The red curve represents the average current calculated each 5 min. The I—V measurement performed after the long time stability test (Fig. 5b) evidenced that the sample had still emitted after 100 h of continuous operation.

The field emission characteristics of randomly oriented W_5O_{14} nanowires are reported. Work function of single W_5O_{14} nanowires was determined by Kelvin microscopy in UHV and ranges from 4.23 to 4.36 eV. Due to relatively low electric resistance and specific surface structure [15], these single crystal nanowires enabled a good current density up to 6.4 mA/cm^2 at very low electric field of about 3 V/μm. The low turn on electric field can be justify from a combined effect of the high enhancement factor and the nanowires work function that is lower than the typical values of CNTs. The long term stability test showed that the nanowires can continuously emit electrons for more than 100 h showing characteristics comparable with carbon nanotubes [24]. The values of the emitted current density are quite higher respect to other tungsten oxide nanoemitters and are fully comparable with the $W_{18}O_{49}$.

All the measurements reported above were taken placing the anode in the central position of the nanowires film in order to avoid possible unwanted effects from the sides of the emitters film. Some measurements on different position of the samples were also taken moving the sample in a range of ± 1.5 mm respect to the central position. The maximum emitting current measeured in the different points has a difference of ± 3 μA respect to the current measured in the central position. Only in two points the maximum current decreased of 6 μA, respect to the 50 μA achieved in the central position. All these results can increase the attention to further investigate these emitter for the realization of uniform large area cathodes. The electrical characteristics of these nanowires are very promising for the realization of long life field emitting cathodes.

Acknowledgments

M. Remskar and J. Jelenc thank Slovenian Research Agency for financing. M. Saqib thanks for financing SIMDALEE2: Marie Curie Initial Training Network (ITN) Grant number 606988 under FP7-PEOPLE-2013-ITN.

References

[1] J. Chen, Y. Dai, J. Luo, Z. Li, S. Deng, J. She, et al., Field emission display device structure based on double-gate driving principle for achieving high brightness using a variety of field emission nanoemitters, Appl. Phys. Lett. 90 (2007) 253105, http://dx.doi.org/10.1063/1.2747192.
[2] A. Sharma, H. Kim, D. Kim, S. Ahn, A carbon nanotube field-emission X-ray tube with a stationary anode target, Microelectron. Eng. 152 (2016) 35–40, http://dx.doi.org/10.1016/j.mee.2015.12.021.
[3] F. Andre, P. Ponard, Y. Rozier, C. Bourat, L. Gangloff, S. Xavier, 7.1: TWT and X-ray devices based on carbon nano-tubes, 2010 IEEE International Vacuum Electronics Conference (IVEC), 2010http://dx.doi.org/10.1109/ivelec.2010.5503591.
[4] G. Ulisse, F. Brunetti, F. Ricci, A. Fiorello, A. Carlo, Cross-bar Design of Nano-Vacuum Triode for high-frequency applications, IEEE Electron Device Lett. 33 (2012) 1318–1320, http://dx.doi.org/10.1109/led.2012.2202367.
[5] S. Young, L. Lai, Field emission properties of ZnO nanosheets grown on a Si substrate, Microelectron. Eng. 148 (2015) 40–43, http://dx.doi.org/10.1016/j.mee.2015.07.012.
[6] L. Vila, P. Vincent, L. Dauginet-De Pra, G. Pirio, E. Minoux, L. Gangloff, et al., Growth and field-emission properties of vertically aligned cobalt nanowire arrays, Nano Lett. 4 (2004) 521–524, http://dx.doi.org/10.1021/nl0499239.
[7] G. Ulisse, F. Brunetti, A. Vomiero, M. Natile, G. Sberveglieri, A. Di Carlo, Hybrid thermal-field emission of ZnO nanowires, Appl. Phys. Lett. 99 (2011) 243108, http://dx.doi.org/10.1063/1.3670331.
[8] Y. ChengO, Zhou, electron field emission from carbon nanotubes, C. R. Phys. 4 (2003) 1021–1033, http://dx.doi.org/10.1016/s1631-0705(03)00103-8.
[9] Y. Huang, H. Chang, H. Chang, Y. Shih, W. Su, C. Ciou, et al., Field emission characteristics of vertically aligned carbon nanotubes with honeycomb configuration grown onto glass substrate with titanium coating, Mater. Sci. Eng. B 182 (2014) 14–20, http://dx.doi.org/10.1016/j.mseb.2013.11.022.
[10] T. Guo, Z. Xu, F. Liu, J. Chen, S. Deng, N. Xu, Synthesis of WO2 Nanowire Arrays on Glass Substrate for Field Emission Application, 2013 26Th International Vacuum Nanoelectronics Conference (IVNC), 2013http://dx.doi.org/10.1109/ivnc.2013.6624753.
[11] J. Zhou, Y. Ding, S.Z. Deng, L. Gong, N.S. Xu, Z.L. Wang, Three-dimensional tungsten oxide nanowire networks, Adv. Mater. 17 (2005) 2107–2110, http://dx.doi.org/10.1002/adma.200500885.
[12] W. Chen, R. Zhan, S. Deng, N. Xu, J. Chen, Anomalous temperature dependence of field emission from W18O49 nanowires caused by surface states and field penetration, J. Appl. Phys. 116 (2014) 133506, http://dx.doi.org/10.1063/1.4896901.
[13] M. Žumer, V. Nemanič, B. Zajec, M. Wang, J. Wang, Y. Liu, et al., The field-emission and current –voltage characteristics of individual W 5 O 14 nanowires, J. Phys. Chem. C 112 (2008) 5250–5253, http://dx.doi.org/10.1021/jp8002273.
[14] J. Bonard, J. Salvetat, T. Stöckli, W. de Heer, L. Forró, A. Châtelain, Field emission from single-wall carbon nanotube films, Appl. Phys. Lett. 73 (1998) 918, http://dx.doi.org/10.1063/1.122037.
[15] M. Remškar, J. Kovac, M. Viršek, M. Mrak, A. Jesih, A. Seabaugh, W5O14 nanowires, Adv. Funct. Mater. 17 (2007) 1974–1978, http://dx.doi.org/10.1002/adfm.200601150.
[16] W. Melitz, J. Shen, A. Kummel, S. Lee, Kelvin probe force microscopy and its application, Surf. Sci. Rep. 66 (2011) 1–27, http://dx.doi.org/10.1016/j.surfrep.2010.10.001.
[17] M. ShiraishiM, Ata, work function of carbon nanotubes, Carbon 39 (2001) 1913–1917, http://dx.doi.org/10.1016/s0008-6223(00)00322-5.
[18] P. Liu, Q. Sun, F. Zhu, K. Liu, K. Jiang, L. Liu, et al., Measuring the work function of carbon nanotubes with thermionic method, Nano Lett. 8 (2008) 647–651, http://dx.doi.org/10.1021/nl0730817.
[19] M.P. Marder, Condensed Matter Physics, Wiley-Interscience, New York, 2000 (ISBN-13: 978–0470617984).
[20] M. Grubbs, M. Deal, Y. Nishi, B. Clemens, The effect of oxygen on the work function of tungsten gate electrodes in MOS devices, IEEE Electron Device Lett. 30 (2009) 925–927, http://dx.doi.org/10.1109/led.2009.2026717.

[21] C. Beleznai, D. Vouagner, J. Girardeau-Montaut, Work function variation during UV laser-induced oxide removal, Appl. Surf. Sci. 138-139 (1999) 6–11, http://dx.doi.org/10.1016/s0169-4332(98)00380-8.
[22] V. Semet, V. Binh, P. Vincent, D. Guillot, K. Teo, M. Chhowalla, et al., Field electron emission from individual carbon nanotubes of a vertically aligned array, Appl. Phys. Lett. 81 (2002) 343, http://dx.doi.org/10.1063/1.1489084.
[23] S. Neupane, M. Lastres, M. Chiarella, W. Li, Q. Su, G. Du, Synthesis and field emission properties of vertically aligned carbon nanotube arrays on copper, Carbon 50 (2012) 2641–2650, http://dx.doi.org/10.1016/j.carbon.2012.02.024.
[24] L. Williams, V. Kumsomboone, W. Ready, M. Walker, Lifetime and failure mechanisms of an arrayed carbon nanotube field emission cathode, IEEE Trans. Electron. Dev. 57 (2010) 3163–3168, http://dx.doi.org/10.1109/ted.2010.2069563.
[25] M. Passacantando, F. Bussolotti, S. Santucci, A. Di Bartolomeo, F. Giubileo, L. Iemmo, et al., Field emission from a selected multiwall carbon nanotube, Nanotechnology 19 (2008) 395701, http://dx.doi.org/10.1088/0957-4484/19/39/395701.
[26] K. Hii, R. Ryan Vallance, S. Chikkamaranahalli, M. Pinar Mengüç, A. Rao, Characterizing field emission from individual carbon nanotubes at small distances, J. Vac. Sci. Technol. B Microelectron. Nanometer. Struct. 24 (2006) 1081, http://dx.doi.org/10.1116/1.2188403.